

# IN-SITU FABRICATION OF FUNCTIONALIZED STARCH MAGNETIC NANOPARTICLES FOR IMMOBILIZATION OF LACCASE

Suhaily Suhaimi<sup>a</sup>, Nardiah Rizwana Jaafar<sup>a\*</sup>, Nashriq Jailani<sup>a</sup>, Roshanida A. Rahman<sup>a</sup>, Norzita Ngadi<sup>a</sup>, Abdul Munir Abdul Murad<sup>b</sup>, Noor Haza Fazlin Hashim<sup>c</sup>, Rosli Md. Illias<sup>a</sup>

## Article history

Received  
12 June 2023  
Received in revised form  
13 August 2023  
Accepted  
17 August 2023  
Published Online  
20 October 2023

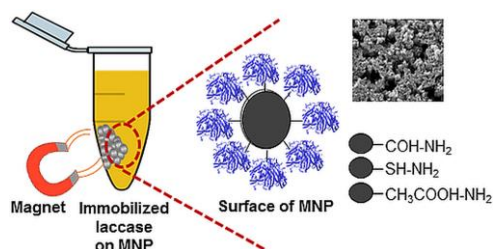
<sup>a</sup>Faculty of Chemical and Energy Engineering, Universiti Teknologi Malaysia, 81310 UTM Johor Bahru, Johor, Malaysia

<sup>b</sup>Department of Biological Sciences and Biotechnology, Faculty of Science and Technology, Universiti Kebangsaan Malaysia, 43600 Bangi, Selangor, Malaysia

<sup>c</sup>Water Quality Laboratory, National Water Research Institute Malaysia (NAHRIM), Ministry of Environmental and Water, Jalan Putra Permai, 43300 Seri Kembangan, Selangor, Malaysia

\*Corresponding author  
nardiah@utm.my

## Graphical abstract



## Abstract

Surface chemistry of magnetic nanoparticles (MNP) is crucial to provide a strong protein-support interaction for the immobilization process. The stability and biocompatibility of the MNP can be structurally enhanced by integrating with organic materials. In this study, MNP from KI/FeCl<sub>3</sub> has successfully synthesized that showed a stronger magnetic strength (72.5 emu/g) compared to common standard precursors, FeCl<sub>2</sub>/FeSO<sub>4</sub> (< 60 emu/g). The synthesized MNP was then incorporated via *in-situ* with functionalized starch; dialdehyde (DAS-MNP), thiol (TS-MNP), and carboxymethyl (CMS-MNP) for Laccase (Lac) immobilization. From docking analysis, CMS-MNP portrayed the highest binding affinity and interacted with highest number of Lac amino acids residues compared to DAS- and TS-MNP. Aligned with this result, immobilized Lac using CMS-MNP achieved the highest recovery activity (80.3%), highly stable at 75 °C for 4 h, and retained more than 50% of its initial activity after 10 cycles. The CMS-MNP-Lac also showed about the same catalytic efficiency with free Lac (1.19 and 1.58 mM<sup>-1</sup>s<sup>-1</sup>, respectively). It is demonstrated that the functional group of the starch-MNP plays a crucial role in attaining a stable immobilized Lac. Therefore, yield a promising biocatalyst to be applied in various fields.

**Keywords:** Magnetic nanoparticles, functionalized starch, laccase, covalent immobilization

## Abstrak

Kimia pada permukaan zarah nano magnetik (MNP) adalah penting untuk menghasilkan interaksi protein-sokongan yang kuat untuk proses imobilisasi. Kestabilan dan keserasianbio MNP boleh dipertingkatkan secara struktur dengan mengintegrasikannya bersama bahan organik. Dalam kajian ini, MNP daripada KI/FeCl<sub>3</sub> telah berjaya disintesis yang menunjukkan kekuatan magnetik yang lebih kuat (72.5 emu/g) berbanding dengan perkursor piawai kebiasaan FeCl<sub>2</sub>/FeSO<sub>4</sub> (< 60 emu/g). MNP yang telah disintesis kemudiannya digabungkan melalui di situ dengan kanji yang telah difungsikan; dialdehid (DAS-MNP), tiol (TS-MNP), dan karboksimetil (CMS-MNP) untuk imobilisasi Lakase

(Lac). Melalui analisis mengedok, CMS-MNP menunjukkan ikatan keafinan tertinggi dan interaksi dengan bilangan sisa asid amino Lac terbanyak berbanding DAS- dan TS-MNP. Sejajar dengan keputusan ini, imobilisasi Lac menggunakan CMS-MNP mencapai aktiviti pemulihan tertinggi (80.3%), kestabilan yang tinggi pada 75 °C selama 4 jam, dan mengekalkan lebih daripada 50% aktiviti awalnya selepas 10 kitaran. CMS-MNP-Lac juga menunjukkan kecekapan pemangkinan yang sama dengan Lac bebas (masing-masing 1.19 dan 1.58 mM<sup>-1</sup>s<sup>-1</sup>). Ini menunjukkan bahawa kumpulan berfungsi kanji-MNP memainkan peranan penting dalam mencapai imobiisasi Lac yang stabil. Oleh itu, menghasilkan biomangkin yang berpotensi untuk diaplikasikan dalam pelbagai bidang.

*Kata kunci:* Zarah nano magnetik, kanji berfungsi, lakase, imobilisasi kovalen

© 2023 Penerbit UTM Press. All rights reserved

## 1.0 INTRODUCTION

Laccase (Lac) from *Trametes versicolor* (EC 1.10.3.2) is a multi-copper-containing oxidase produced by living organisms which catalyses one-electron (e<sup>-</sup>) oxidations of diverse organic and inorganic substrates [1]. It is known to have the ability to decolorize textile dyes, participate in delignification of lignocellulosic materials and remove antibiotic wastes [2]. Nevertheless, industrialized operation of enzyme in its free form is hindered by a few factors including high production cost, inconvenient in separation and lack of enzymatic effectiveness after one cycle. To address these issues, enzyme immobilization technique is introduced as an alternative to improve the enzymatic properties [3].

Generally, adsorption on a surface [4], covalent bonding to a support [5], entrapment in polymer gel [6], and cross-linked aggregation [7] are commonly used in Lac immobilization. Moreover, different immobilization support offers different physical and chemical properties. For example, immobilized enzyme onto a porous support usually has remarkably high enzyme recovery. However, it is often associated with substrate diffusion limitation [3]. Other than that, the use of polymer gels could certainly increase enzyme stability but these supports exhibited swelling and easily broken down into pieces making them unsuitable for enzymes that require prolonged reaction time [8]. Magnetic nanoparticles (MNP) is receiving considerable attention as it exhibits great performance for particle size ranging from 10 to 100 nm [9]. Besides, the fact that MNP offers large specific surface area as well as quick response towards magnetic field adds its appeal for use in enzyme immobilization. However, unmodified MNP has a tendency to aggregate, resulting in larger particle size, and is easily oxidized in air [10]. Thus, the surface of the MNP usually undergoes modification to counter these issues.

Grafting or coating the MNP with organic and inorganic materials allows structural tuning for stability and biocompatibility of the MNP [11]. In recent years, organic polysaccharides such as starch, chitosan, dextran, maltodextrin and fucan have been used in

fabricating the MNP [12]. Starch is a polymeric carbohydrate consists of large number of glucoses linked with  $\alpha$ -1,4 and  $\alpha$ -1,6-glycosidic bonds. It is a green renewable polysaccharide source that has good biocompatibility [13]. Thus, starch has emerged as one of the promising materials in fabricating eco-friendly MNP. Besides, starch offers vast applications due to the presence of three hydroxyl groups at 2, 3 and 6 carbon atoms in each anhydroglucose unit, which enable chemical modification to various functional groups [14]. The incorporation of functionalized starch does not only rectify the downsides of unmodified MNP but also acts as bioligand which assists in the attachment of enzyme in enzyme immobilization.

Studies on enzyme immobilization using MNP as a support thus far have solely focused on only one type of functional group; aldehyde-MNP using glutaraldehyde [15], thiol-MNP using N-Hydroxysuccinimide ester [16], and carboxymethyl-MNP using Na,Na-Bis(carboxymethyl)-L-lysine hydrate [17]. The aldehyde, thiol, and carboxymethyl are among chemical groups that bind to the nucleophile of the enzyme with high recovery and stability [18]. It can be concluded that with changes or addition of functional group can affect the surface chemistry of a support which gives strong interaction and high stability of immobilized enzyme. To the best of our knowledge, a comparative study between the best three functional groups (aldehyde, thiol and carboxymethyl) for Lac immobilization has yet to be well studied.

Therefore, the aim of this study is to determine the type of precursor producing the strongest magnetic strength and to determine the preferential functional groups for Lac immobilization. Herein, MNP was synthesized where a total of six precursors were screened to yield the highest magnetic strength. Following this, functionalized starch; dialdehyde (DAS), thiol (TS), and carboxymethyl (CMS) were incorporated with the synthesized MNP for the development of Lac immobilization. The results showed that, fabrication of MNP from KI/FeCl<sub>3</sub> which has never been used in any enzyme immobilization application, produced the strongest magnetic

strength. Besides, the incorporation of CMS with MNP successfully increased the biocompatibility, resulting higher recovery activity, stability, and reusability of Lac in comparison with DAS and TS. The experimental data was supported with the analysis from molecular docking that portrayed CMS-MNP has the highest binding affinity and farthest distance interaction with Lac active site. This suggests that the immobilization of Lac on CMS-MNP is proven to generate promising performance of biocatalyst for various application.

## 2.0 METHODOLOGY

### 2.1 Synthesis of Magnetic Nanoparticles (MNP)

The MNP was synthesized according to previous study by Sulistyarningsih *et al.* [19] with some modification. Six types of precursors such as copper (II) chloride ( $\text{CuCl}_2$ ), zinc (II) chloride ( $\text{ZnCl}_2$ ), cobalt (II) chloride ( $\text{CoCl}_2$ ), nickel chloride ( $\text{NiCl}_2$ ), potassium iodide (KI) and ferrous sulphate ( $\text{FeSO}_4$ ) was mixed with iron (III) chloride ( $\text{FeCl}_3$ ) using molar ratio of 2:1 in total volume of 25 mL distilled water. Then, 25% (w/v) of sodium hydroxide was added dropwise at 50 °C under constant stirring until the pH of the solution increase to 11. After 3 h of aging, the product was collected by external magnet through magnetic decantation. The synthesized product was continuously washed and rinsed with distilled water to neutral pH and dried at 60 °C in an oven for overnight. Among the precursors, only  $\text{NiCl}_2$ , KI and  $\text{FeSO}_4$  were successfully retrieved by using the external magnet. Thus, these three precursors were tested with Vibration Sample Magnetometer (VSM) to determine the highest magnetic strength. The magnetization applied field (1.4 Tesla) was measured at room temperature. The selected precursor with the highest magnetic strength was further investigated by varying the molar ratio (0.5, 1, 2 and 3) with  $\text{FeCl}_3$  [20].

### 2.2 Preparation of Functionalized Starch and Functionalized Starch MNP

Dialdehyde starch (DAS), thiolate starch (TS) and carboxymethyl starch (CMS) was functionalized by chemical modification. Details can be found in Supplementary Materials.

To prepare DAS-, TS-, and CMS-MNP, each of the functionalized starch was dissolved in distilled water separately and added into magnetic solution at temperature of 30 °C. Then, 25% (w/v) of NaOH solution was added dropwise until the pH reached pH 11. After 3 h of aging, the functionalized starch MNP was collected by external magnetic, washed with distilled water until it reached pH 7 and finally dried at 60 °C for overnight.

### 2.3 Immobilization of Lac onto Functionalized Starch Magnetic Nanoparticles

The immobilization of commercial Lac was optimized by manipulating immobilization parameters via one factor at a time (OFAT) approach. The details on immobilization process, determination of Lac assay, protein content, and recovery activity can be found in Supplementary Materials.

### 2.4 Computational Analysis, Biological and Physical Characterization

Details on computational analysis, biological characteristics of free and immobilized Lac (thermal stability, kinetics study, and reusability) and physical characterization on CMS-MNP (XRD, TGA, ICP-OES, FTIR, and SEM) can be found in Supplementary Materials.

## 3.0 RESULTS AND DISCUSSION

### 3.1 Development of MNP

The MNP was developed via co-precipitation method. Ferric chloride ( $\text{FeCl}_3$ ) solution was mixed with various type of precursors such as copper (II) chloride ( $\text{CuCl}_2$ ), zinc (II) chloride ( $\text{ZnCl}_2$ ), cobalt (II) chloride ( $\text{CoCl}_2$ ), nickel chloride ( $\text{NiCl}_2$ ), potassium iodide (KI) and ferrous sulphate ( $\text{FeSO}_4$ ). The synthesized MNP using these precursors were analyzed based on the magnetic strength. Preliminary results showed out of six precursors that were screened, the MNP synthesized from the mixture of  $\text{FeCl}_3/\text{CuCl}_2$ ,  $\text{FeCl}_3/\text{ZnCl}_2$ , and  $\text{FeCl}_3/\text{CoCl}_2$  have failed to be attracted towards the external magnet. This reveals that the MNP synthesized from these precursors have very slow response towards external magnet (Figure 1). According to Harada *et al.* [21], the magnetic strength of the MNP tend to reduce by the periodic arrangement due to the strong dependence on the cation magnetic moment. Thus,  $\text{Cu}^{2+}$ ,  $\text{Zn}^{2+}$ , and  $\text{Co}^{2+}$  are among the cation that would produce a weak attraction towards the external magnet. Due to this, the synthesized MNP from these three types of precursors are unsuitable to be used for the application of enzyme immobilization in this study as it would cause inefficient enzyme separation process. The mixture of  $\text{FeCl}_3/\text{NiCl}_2$ ,  $\text{FeCl}_3/\text{KI}$ , and  $\text{FeCl}_3/\text{FeSO}_4$  were able to be attracted towards external magnet thus were further examined using Vibration Sample Magnetometer (VSM) and the result was presented in the form of hysteresis loop as shown in Figure 1(A).

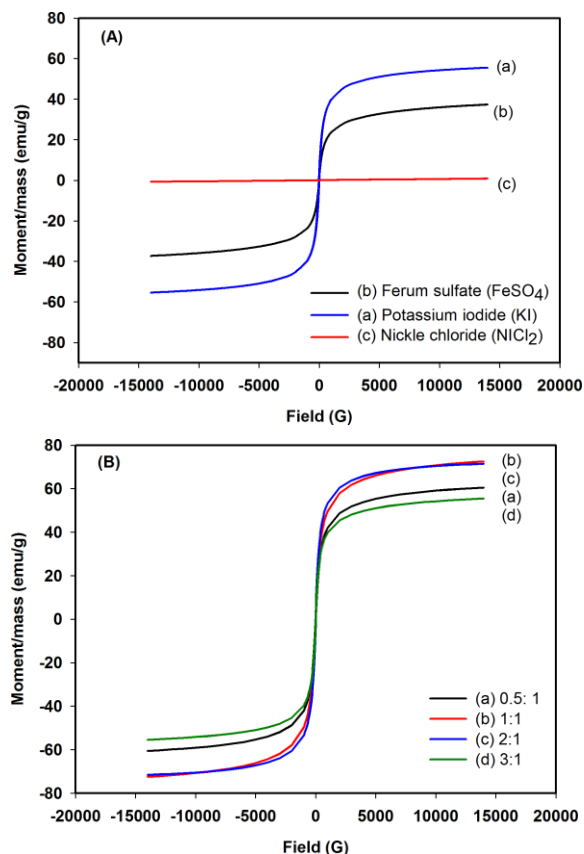


**Figure 1** Magnetization of (A) different type of precursor and (B) different molar ratio of KI/FeCl<sub>3</sub>

The types of precursor used in the fabrication of MNP clearly influenced the hysteresis loop. This is due to change in distribution of cation of the precursor during the precipitation process [22]. Based on the loop, KI (55.456 emu/g) showed the highest magnetization saturation ( $M_s$ ) followed by FeSO<sub>4</sub> and NiCl<sub>2</sub> (37.311 and 0.771 emu/g, respectively). Since co-precipitation of KI/FeCl<sub>3</sub> recorded the highest magnetization saturation, hence, mixture of KI/FeCl<sub>3</sub> was selected for further optimization to enhance the magnetic property. The molar concentration of KI was varied from 0.5 to 3 mol while the concentration of FeCl<sub>3</sub> was fixed to 1 mol and the results were illustrated in Figure 1(B). Based on the figure, the magnetization saturation when using molar ratio of 1:1 (72.54 emu/g) was higher compared to molar ratio of 2:1 which was 71.53 emu/g. According to Mizutani *et al.* [23] molar ratio is one of the important operating factors which affects the nucleation-growth rate during the synthesis of MNP. This, consequently, affects the crystallinity of the particles as well as the magnetic saturation [24]. In this study, molar ratio of 1:1 was used to incorporate with functionalized starch in the next section. It is noteworthy that fabrication of MNP using KI/FeCl<sub>3</sub> in this study was the first one to be reported for enzyme immobilization, while previous studies used

Fe(II)/Fe(III) mixture as a standard protocol [9]. The magnetization saturation value in this study was higher compared to previous studies where majority reported less than 60 emu/g [25]–[28]. The low magnetization saturation, consequently affecting the recovery of the immobilized enzyme due to weak magnetic attraction during separation process.

### 3.2 Preparation and Characterization of Functionalized Starch

Dialdehyde (DAS), thiolate starch (TS), and carboxymethyl starch (CMS) was functionalized on soluble starch through oxidation process using sodium periodate, thioglycolic acid and monochloroacetic acid, respectively. The oxidation parameters such as concentration, temperature and time for the three functional groups were investigated. The results were tabulated in the Table S2. From the results, final aldehyde content was 37.03%, thiol content was 58.1%, and carboxymethyl content was 32%, respectively.

The FTIR spectra for native starch, DAS, TS, and CMS are shown in Figure 2. For native starch (Figure 2A), the main functional groups are the secondary -OH groups at the position of C<sub>2</sub> and C<sub>3</sub>. The broad peak at 3334 cm<sup>-1</sup> portrays the -OH stretching present in the starch structure [29]. To confirm the presence of aldehyde functional group, peak at 1689 cm<sup>-1</sup> was observed in the FTIR spectra (Figure 2B). The peak was not as intense as in the study by Yu *et al.* (2010) [30] due to smaller amount of aldehyde produced in this study. Other than that, the peak of C-O bond stretching in C-O-H group in the anhydro glucose ring of starch was approximately at 1149 cm<sup>-1</sup>. The weak peak at 2510 cm<sup>-1</sup> contributes to the S-H bond for thiol group in starch (Figure 2C). As for CMS (Figure 2D), new peaks occurred at 1573 and 1476 cm<sup>-1</sup> indicating the substitution of COO<sup>-</sup> group on the molecular chain producing unsymmetrical and symmetrical stretching vibration, respectively [31].

The morphological structure was viewed by using SEM at magnification of 500 times (Figure 2). The figure shows that after the native starch (Figure 2A) was oxidized to DAS, the starch particles changed from smooth granular shape into oblate spheres with collapse structure in the middle of the particles (Figure 2B) indicating that the amorphous and crystal structure of the starch granules were discrete in the interior and outer region [32]. Meanwhile, TS (Figure 2C) portrays aggregation of the starch particles at the same magnification which is consistent with the study reported by Das and Das [33]. As for CMS (Figure 2D), the granules have indented surface and have become shrunken, wrinkled, and certain particles were broken. This observation is similar to a study by Li, Mujiyambereb, and Liu [34]. Generally, starch granules that undergo chemical modification would display disrupted structures. Hence, resulting in the shape of DAS, TS and CMS as shown in this study. Both FTIR and SEM analysis from Figure 2 proved that starch has successfully been functionalized to

aldehyde, thiol, and carboxymethyl. These functionalized starches were incorporated with the synthesized MNP and their performance as support for Lac immobilization were evaluated in the next section.

### 3.3 Immobilization of Lac on Functionalized Starch MNP

Concentration of functionalized starch used in the preparation of MNP is crucial for the immobilization of Lac as well as magnetic strength of the MNP. The attraction of MNP with the external magnet decrease when higher concentration of functionalized starch was used and this reflect in very weak/no magnetic strength of the nanoparticles [35]. Figure 2 shows the recovery activity of Lac at different concentrations of functionalized starch. The concentration for TS-MNP and CMS-MNP ranged from 0.06 to 1.0%, whereas DAS-MNP used functionalized starch at concentrations of 0.06 to 0.6% (Figure 2).

The highest recovery activity achieved was 54.1% when the concentration of 0.2% CMS-MNP-Lac was used (Figure 2). Meanwhile, its lowest recovery activity was recorded at 0.06% concentration with the recovery activity of 42.9%. As for DAS-MNP-Lac and TS-MNP-Lac, the highest recovery activity was at concentration 0.4% and 0.2% with recovery activity of 59% and 61.5%, respectively. The concentration of functionalized starch is an important factor; whereby if the concentration is too low, low attachment can occur resulting less efficient Lac immobilization. However, excess functionalized starch support can result in a complete loss of enzyme flexibility thus affecting the activity recovery. Figure 2 showed that further increase in the functionalized starch concentration resulted in a decrease in enzyme recovery which might be due to the compact linkage between Lac and MNP that affects the diffusion of substrate into the active site of the enzyme [36].

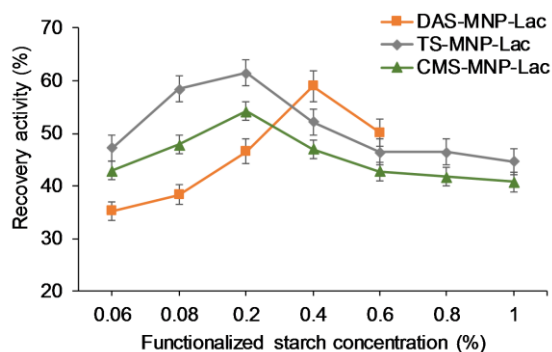


**Figure 2** Effect functionalized starch concentration on recovery activity

The effect of Lac loading on Lac immobilization was determined by varying the Lac concentration

from 1 to 6 mg/mL (0.083 to 0.110 U/mL). The results in Figure 3 indicated that the recovery activity was increased as the enzyme concentration increased from 1 to 3 mg/mL for DAS-MNP-Lac, while TS-MNP-Lac and CMS-MNP-Lac increased from 1 to 5 mg/mL. This shows that the increment in Lac concentration enhanced the driving force for the binding of Lac onto the MNP. CMS-MNP-Lac showed the highest recovery activity (80.3%, 4.060 U/g) at Lac concentration of 3 mg/mL, meanwhile, the highest activity recorded for DAS- and TS-CMP-Lac were 70.4% (3.459 U/g), and 74.4% (3.629 U/g), respectively at 5 mg/mL of Lac. Increasing Lac concentration from 3 to 6 mg/mL for CMS-MNP-Lac immobilization resulted a decreased in its activity recovery while DAS- and TS-MNP-Lac showed a stagnant activity recovery at increasing Lac concentration from 5 to 6 mg/mL. This could be explained by the oversaturation of enzyme on the surface of functionalized starch MNP. The excessive enzyme molecules crowding on the surface of the immobilization support has proven to reduce enzyme activity due the protein-protein interaction and inhibit flexible structure of enzyme which leads to spatial restriction, limited active site accessibility and thus the inactivation of enzyme [37]. The overcrowding condition may also cause difficulty in modulating suitable conformation for the binding and releasing of the substrate and product molecules, respectively [38].

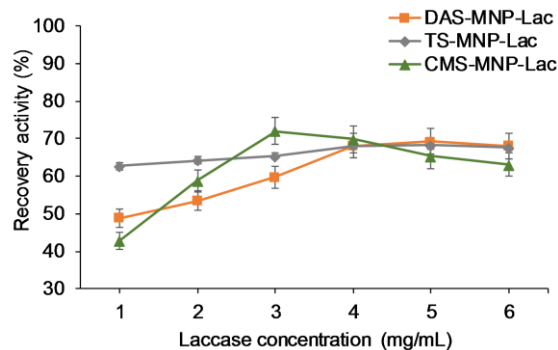


**Figure 3** Effect of Lac MNP concentration on recovery activity

The immobilization of Lac was performed at time ranging from 1 to 5 h. The result presented in Figure 4 showed that DAS-MNP-Lac requires longer immobilization time (4 h) to achieve the highest recovery activity (68.8%) in comparison with CMS-MNP-Lac which requires only 2 h to achieve 72.7% of activity recovery. As for TS-MNP-Lac, the highest recovery activity recorded was at 2 h with 64.9%. The increase in contact time increased the amount of enzyme interacting on the surface of MNP resulting in improvement of Lac immobilization. Even though some of immobilization processes take shorter time for the enzyme to be immobilized, the interaction of enzyme and support is a time dependable process in which its proper binding of enzyme is needed,

otherwise immobilization will not occur [39]. Nevertheless, prolong incubation time increases the interaction of Lac with the MNP hence making the structure becoming more compact, consequently, introduces substrate diffusion limitation. This explained the decreased of recovery activity once they have reached the optimized immobilization time.

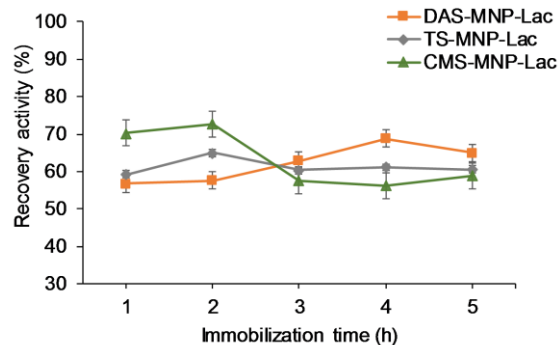


**Figure 4** Effect of immobilization time on recovery activity

The effect of mass of functionalized starch MNP was investigated from 1 to 5 mg as shown in Figure 5. Based on the result, the efficiency of Lac immobilization was affected by the mass of DAS-MNP, TS-MNP, and CMS-MNP. The highest recovery activity showed by CMS-MNP-Lac (80.3%) followed by TS-MNP-Lac (74.4%) when using 4 mg functionalized starch MNP, respectively. Meanwhile, the highest activity recovery recorded for DAS-MNP-Lac was 67.5% when 2 mg of functionalized starch MNP was used. From Figure 5, the increase in recovery activity as the mass of functionalized starch MNP increased in CMS-MNP-Lac is due to the availability of the surface for the binding of Lac [40]. This result is similar with a study reported by Mohamed *et al.* [41] who varied unmodified MNP onto horseradish peroxidase (HRP). In the study, the HRP required 200 mg of MNP to achieved highest residual activity (90%). In this current study showed that considerably high activity recovery is achieved with small amount of functionalized starch MNP.

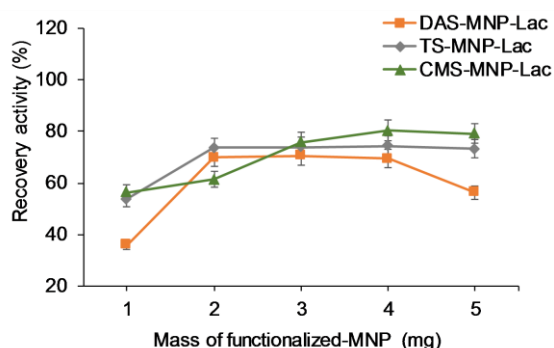


**Figure 5** Effect of mass of functionalized starch MNP on recovery activity

### 3.4 Molecular Docking Analysis

For immobilization of Lac, strong interaction between enzyme and functional group on the surface of MNP is needed to produce a stable immobilized Lac. In this study, molecular docking technique was employed to predict the binding of aldehyde, thiol and carboxymethyl as ligands with Lac as receptor. Table 2 shows the predicted binding energy and predicted Lac residues involved in the interaction with the functional groups examined in this study. Among the three functional groups, CMS showed the lowest predicted binding energy in comparison with DAS and TS. Low predicted binding energy is associated with low equilibrium dissociation resulting in stronger binding affinity [42]. Other than that, CMS was predicted to interact with 8 amino acid residues in Lac which offer greater strength in interactions than DAS and TS. This predicted result was in agreement with the experimental study which has been conducted in the previous section.

In order to have an effective catalytic reaction of immobilized enzyme, substrate should be able to diffuse and reach the active site of the immobilized enzyme easily. The affinity of substrate towards the active site depends on the enzyme's position and orientation on the immobilization support [43]. Figure 3 shows the interaction distance between Lac active site residues (His-395, His-458 and Cys-453) (shown in yellow) with the functionalized starch DAS, TS, and CMS (shown in blue). Based on Figure 3, it was estimated that the distance for CMS was the farthest (11.0 Å) followed by DAS (8.9 Å) and TS (8.0 Å). The interaction distance plays a significant role that directly affect kinetic parameters for immobilized enzyme in which, the farther the distance, the lesser the substrate diffusion limitation during enzymatic reaction [44].

### 3.5 Biochemical Characterization of Free and Immobilized Lac

#### 3.5.1 Thermal Stability

The thermal stability of free Lac, DAS-MNP-Lac, TS-MNP-Lac and CMS-MNP-Lac were determined at different temperatures ranging at different time intervals as presented in Figure 4. The temperature profile at 30 °C in Figure 4A revealed that both free and immobilized Lac displayed almost similar stability trends and retained more than 70% relative activity after 5 h. Nonetheless, at 50 °C, the stability of DAS-MNP-Lac and TS-MNP-Lac dropped to 65 and 63% while free Lac and CMS-MNP-Lac, both retained 74 and 77% of their relative activity (Figure 4B). At 75 °C, the relative activity of DAS-MNP-Lac and TS-MNP-Lac dropped significantly after 1.5 h of incubation time and only managed to retain less than 10% of their relative activity after 4 h incubation. In comparison, free Lac and CMS-MNP-Lac displayed higher thermal resistance as both exhibited higher than 30% of their relative activity after 4 h of incubation. The overall

decrease of relative activity for the immobilized Lac might be due to the leaching of iron in magnetic nanoparticles itself. This is because, when Inductively Coupled Plasma – Optical Emission Spectroscopy (ICP-OES) analysis was conducted, more than 400 µg/L trace of iron was found in the residue after incubation at 75 °C which indicated that the iron was not able to tolerate high temperature for an extended period of time (Table 3). The leaching of iron has caused most of the immobilized Lac to detach from the MNP and directly affected the thermal stability, hence the low relative activity.

Nevertheless, between the three types of functionalized starch MNP studied in this report, CMS-MNP is far more stable than DAS and TS. This was attributed to the fact that carboxymethyl functional group was predicted to have the strongest binding with enzyme Lac in comparison to aldehyde and thiol functional groups (Table 2). Moreover, the thermal stability of CMS-MNP-Lac is related to the interaction where carboxymethyl groups offer greater stability for the Lac in terms of structural rigidity and less susceptible to thermal changes in conformation compared to aldehyde and thiol groups. The structural perseverance thereby retained the active site of Lac from denaturation. This trend was also in agreement with a study by Fortes *et al.* [45] which reported that the relative activity of free and Lac immobilized on silica coated magnetic nanoparticles remained consistent after 5 h of incubation in 60 °C.

Thermal deactivation analysis of free Lac, DAS-MNP-Lac, TS-MNP-Lac and CMS-MNP-Lac was determined by plotting pseudo-first order-plot graph as shown in Figure 5. The thermal deactivation kinetics such as deactivation constant ( $k_d$ ) and half-life ( $t_{1/2}$ ) for free and immobilized Lac are tabulated in Table 1. Based on the results, the value of  $k_d$  showed no significant difference at temperatures of 30 °C and 50 °C. Meanwhile, at temperature 75 °C, CMS-MNP-Lac showed about the same  $k_d$  value with free Lac (0.276 h<sup>-1</sup> and 0.286 h<sup>-1</sup>, respectively). TS-MNP-Lac (0.633 h<sup>-1</sup>) showed a higher  $k_d$  value followed by DAS-MNP-Lac (0.931 h<sup>-1</sup>). Smaller  $k_d$  value indicates that CMS-MNP-Lac is not prone to rapid degradation at higher temperature compared to DAS-MNP-Lac and TS-MNP-Lac. Corroborating these results, CMS-MNP-Lac showed a similar trend for half-life ( $t_{1/2}$ ) indicating that CMS-MNP-Lac has the slowest enzyme deactivation rate. This similar trend might be due to the strong interaction of Lac with the carboxymethyl group on the surface of the MNP and the rigidity of the structure that able to withstand at high temperature.

**Table 1** Thermal deactivation constants of free and immobilized Lac

Enzyme	T (°C)	$k_d$ (h <sup>-1</sup> )	$t_{1/2}$ (h)
Free Lac	30	0.065	10.647
	50	0.067	10.299
	75	0.220	3.148

Enzyme	T (°C)	$k_d$ (h <sup>-1</sup> )	$t_{1/2}$ (h)
DAS-MNP-Lac	30	0.075	9.304
	50	0.078	8.852
	75	0.692	1.002
TS-MNP-Lac	30	0.079	8.785
	50	0.086	8.069
	75	0.798	0.869
CMS-MNP-Lac	30	0.061	11.326
	50	0.064	10.847
	75	0.240	2.894

### 3.5.2 Kinetic Study of Free and Immobilized Lac

The catalytic efficiency of the immobilized and free Lac was studied by determining the reaction rate at different ABTS concentrations. The rates of reaction were fit into Lineweaver-Burk plot in order to obtain Michaelis-Menten kinetic parameters. Table 2 shows that  $V_{max}$  value of CMS-MNP-Lac is closer to free Lac by 1.09-fold in comparison with DAS-MNP-Lac and TS-MNP-Lac with 1.63 and 1.19-fold, respectively. The value of  $V_{max}$  can be depicted as the maximum rate of reaction when the active site is saturated with substrate. From the previous report, the value of  $V_{max}$  for immobilized enzyme would be slightly lower compared to free enzyme. Furthermore, the recovery activity was also contributing factor for lower  $V_{max}$  showed by DAS-MNP-Lac and TS-MNP-Lac in this study.

**Table 2** Kinetic parameters for free and immobilized Lac

Kinetic parameter	Free Lac	DAS-MNP-Lac	TS-MNP-Lac	CMS-MNP-Lac
$V_{max}$ (µmol mL <sup>-1</sup> min <sup>-1</sup> )	4.28	2.62	3.58	3.92
$K_m$ (mM)	2.8	3.61	3.71	3.40
$k_{cat}$ (s <sup>-1</sup> )	4.42	2.7	3.70	4.05
$k_{cat}/K_m$ (mM <sup>-1</sup> s <sup>-1</sup> )	1.58	0.75	1.0	1.19

On the other hand, the  $K_m$  value of the CMS-MNP-Lac was 3.4 mM, which was slightly higher than free Lac with 2.8 mM. Nevertheless, DAS-MNP-Lac and TS-MNP-Lac exhibited the highest  $K_m$  values among all. The interaction of Lac with substrate are specified by the  $K_m$  value in which small  $K_m$  value indicated good substrate affinity at the active site. The results presented in Table 2 showed that immobilization influenced structural conformation, resulting in slightly low affinity for substrate as compared to free Lac, where the catalytic site could directly undergo reaction without any hindrance. This result is in accordance with the docking analysis shown in Figure S3 in which both DAS-MNP-Lac and TS-MNP-Lac exhibited the nearest distance to the active site. Thus, the orientation of the immobilized Lac might limit the mass transfer diffusion of the substrate to the active site of the enzyme, hence resulting in high  $K_m$  value. In contrast with CMS-MNP-

Lac, lower  $K_m$  value was probably due to farther interaction distance with the active site of Lac that prevent the limitation of substrate diffusion. Furthermore, DAS-MNP-Lac and TS-MNP-Lac have lower value of  $k_{cat}$  demonstrating that the catalysis rate of the immobilized enzyme is slower than the free enzyme thus proving that orientation of the enzyme on a support is crucial in immobilization.

### 3.5.3 Reusability of Immobilized Lac

The reusability of the DAS-MNP-Lac, TS-MNP-Lac and CMS-MNP-Lac was tested repetitively up to 10 cycles using ABTS at 25 °C and was recovered using magnetic separation. The operational stability of immobilized Lac is shown in Figure 6. The trend showed a slight decrease in activity for all three functionalized starch MNP after each cycle. However, the immobilized Lac exhibited good activity in which CMS-MNP-Lac retained more than 52% of its initial activity followed by DAS-MNP-Lac with 45% and TS-CMS-Lac with 40% throughout the 10 cycles. The reusability in this study is comparatively higher than a study conducted by Chen *et al.* [46] which reported that residual activity of immobilized Lac on amino functionalized MNP retained about 40% after only 8 cycles. The application of MNP in enzyme immobilization is attractive considering that the enzyme recovery simply requires magnetic field to separate the immobilized enzyme from reaction mixture. Moreover, the use of magnet eliminates the need for centrifugation in separation step which often leads to structural loss of enzyme, hence causing enzyme inactivation after each cycle [47].

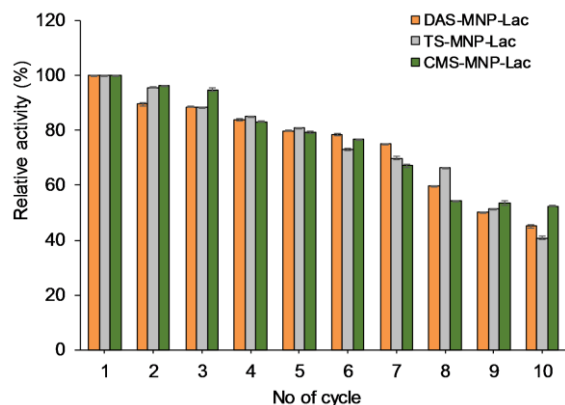


**Figure 6** Reusability of Lac immobilized on different functionalized starch MNP

### 3.6 Physical Characterization of MNP, CMS-MNP and CMS-MNP-Lac

Comparing DAS, TS and CMS-MNP in the earlier sections, the latter yielded positive results for the immobilization of Lac. This section is therefore focused more on the physical characterization of the CMS-MNP. The XRD patterns of MNP and CMS-MNP are shown in Figure 6(A). The characteristic peaks

which occurred in the spectrum of MNP at  $2\theta = 31.56^\circ, 35.48^\circ, 45.34^\circ, 53.64^\circ, 57.22^\circ$  and  $62.78^\circ$ , correspond to (2 2 0), (3 1 1), (4 0 0), (4 2 2), (5 1 1), and (4 4 0), respectively [48]. These diffraction peaks are identical with the standard spectrum of  $Fe_3O_4$ , and related crystal matched with JCPDS No. 82-1553. When comparing spectrum of MNP with that of CMS-MNP (Figure 6B), it could be seen that CMS-MNP was missing one peak at  $53.64^\circ$ . Based on this finding, the MNP's crystalline structure had shown to change after interacted with CMS. Besides, after the calculation of crystalline size for both MNP and CMS-MNP using Debye Scherrer equation [49], the MNP size was 7.8 nm which was smaller in comparison with CMS-MNP which was 9.97 nm. This demonstrated minor changes in crystallinity following CMS adjustment.

TGA were performed at temperature ranging from 30 – 900 °C as shown in Figure 7. The thermogram profile at 30 °C to 120 °C displays that CMS-MNP-Lac exhibited slight weight loss behavior of approximately 6.43 % in comparison with CMS-MNP with 5.4 %. This shows that physically bonded water molecules were evaporated, and unreacted constituents were lost at this phase[50]. Meanwhile, at temperature  $>250$  °C both components showed a decrease in the weight percentage mainly due to the decomposition of organic compounds such as starch in the MNP [51]. However, extensive decomposition (14%) could be seen for CMS-MNP-Lac whereby it contributed to the pyrolysis of Lac which is also reported by Wang *et al.* [52]. Maximum decomposition temperature ( $T_{max}$ ) of CMS-MNP and CMS-MNP-Lac were at 297 and 267 °C, respectively. This suggests that thermal stability of the CMS-MNP after the immobilization process decreased which might be attributed to the slight change in crystallinity structure observed in XRD analysis in the previous section. This observation is in agreement with the thermal stability of CMS-MNP-Lac that showed a slightly lower relative activity compared to free Lac after incubation at 75 °C for 4 h.

TEM images and SEM-EDX of MNP and CMS-MNP were visualized as shown in Figure 8. The MNP (Figure 8A) had a typical spherical morphology with an average size of 10.3 nm. After the incorporation of CMS, the particles of CMS-MNP (Figure 8B) maintained the shape and had an average size of 14.8 nm. This reveals that the presence of CMS in the MNP did not significantly affect the size of the particles. Similar changes in size before and after modification of MNP were also reported from previous study where the functionalized MNP with tetraethyl orthosilicate and (3-Aminopropyl)triethoxysilane affected the size of the particles [53]. These sizes, however, were slightly bigger than the crystalline sizes calculated from XRD analysis. This could be due to the presence of multiple crystal domain in one particle. Nevertheless, the size obtained in this study is within the range of nanoparticle size (between 1 – 100 nm) as described by Ali *et al.*, [54]. The nano size of the particles



provides large specific surface area for the effective attachment of Lac in immobilization which reflected the recovery activity in Section 3.3. Finally, through a SEM-EDX micrographs analysis, the surface of CMS-MNP-Lac (Figure 8D) was rougher in comparison with CMS-MNP (Figure 8C) which indicated that there was Lac presence on the CMS-MNP. The existence of N element from amino acid residues in elemental composition of CMS-MNP-Lac further confirmed the presence of Lac. It was also observed that CMS-MNP shown to have an increase in cavity compared to MNP only. Increasing in porosity showed by the CMS-MNP probably resulting in large surface area thus corroborated with the high recovery activity of CMS-MNP-Lac immobilization. Furthermore, the presence of high cavities also can be the contributing factor of its catalytic efficiency. In this study, CMS-MNP-Lac possessed about the same catalytic efficiency as free Lac.

#### 4.0 CONCLUSION

Magnetic nanoparticles (MNP) synthesized from KI/FeCl<sub>3</sub> was successfully prepared and managed to obtain the highest magnetic strength which significantly assisted in the recovery of immobilized laccase (Lac). The incorporation of the MNP with carboxymethyl starch (CMS) has successfully increased the biocompatibility with Lac via covalent bonding whereby, the CMS-MNP-Lac showed the highest recovery activity, thermal stability, and reusability compared to dialdehyde starch (DAS) and thiolate starch (TS). In this study, CMS portrayed the highest binding affinity with Lac and has the farthest interaction distance with Lac active sites as demonstrated in molecular docking analysis which could reduce substrate diffusion limitation after immobilization. Thus, with the easy magnetic separation step using MNP, the application in various industries especially in bioremediation is beneficial since filtration or centrifugation that frequently affects the structure of immobilized enzyme could be avoided.

#### Conflicts of Interest

The author(s) declare(s) that there is no conflict of interest regarding the publication of this paper.

#### Acknowledgement

This work was supported by Universiti Teknologi Malaysia [Grant Number: Q.J130000.2409.08G54].

#### References

- [1] R. Mehra, J. Muschiol, A. S. Meyer, and K. P. Kepp. 2018. A Structural-chemical Explanation of Fungal Laccase Activity. *Sci. Rep.* 8(1): 1-16.
- [2] S. Datta, R. Veena, M. S. Samuel, and E. Selvarajan. 2021. Immobilization of Laccases and Applications for the Detection and Remediation of Pollutants: A Review. *Environ. Chem. Lett.* 19(1): 521-538. <https://doi.org/10.1007/s10311-020-01081-y>.
- [3] A. Basso and S. Serban. 2019. Industrial Applications of Immobilized Enzymes-A Review. *Mol. Catal.* 479(September): 110607. <https://doi.org/10.1016/j.mcat.2019.110607>.
- [4] R. O. Cristóvão et al. 2011. Enzymatic Immobilization of Commercial Laccase onto Green Coconut Fiber by Adsorption and its Application for Reactive Textile Dyes Degradation. *J. Mol. Catal. B Enzym.* 72: 6-12. <https://doi.org/10.1016/j.molcatb.2011.04.014>.
- [5] L. Lonappan et al. 2018. Covalent Immobilization of Laccase on Citric Acid Functionalized Micro-biochars Derived from Different Feedstock and Removal of Diclofenac. *Chem. Eng. J.* 351(June): 985-994. <https://doi.org/10.1016/j.cej.2018.06.157>.
- [6] J. Gill, V. Orsat, and S. Kermasha. 2018. Optimization of Encapsulation of a Microbial Laccase Enzymatic Extract using Selected Matrices. *Process Biochem.* 65(November): 55-61. <https://doi.org/10.1016/j.procbio.2017.11.011>.
- [7] J. Hong, D. Jung, S. Park, Y. Oh, K. K. Oh, and S. H. Lee. 2021. Immobilization of Laccase via Cross-linked Enzyme Aggregates Prepared using Genipin as a Natural Cross-linker. *Int. J. Biol. Macromol.* 169: 541-550. <https://doi.org/10.1016/j.ijbiomac.2020.12.136>.
- [8] C. Horn, D. Pospiech, P. J. Allertz, M. Müller, K. Salchert, and R. Hommel. 2021. Chemical Design of Hydrogels with Immobilized Laccase for the Reduction of Persistent Trace Compounds in Wastewater. *ACS Appl. Polym. Mater.* 3(5): 2823-2834. <https://doi.org/10.1021/acsapm.1c00380>.
- [9] M. Bilal, Y. Zhao, T. Rasheed, and H. M. N. Iqbal. 2018. Magnetic Nanoparticles as Versatile Carriers for Enzymes Immobilization: A Review. *Int. J. Biol. Macromol.* 120: 2530-2544. <https://doi.org/10.1016/j.ijbiomac.2018.09.025>.
- [10] M. Mahdavi et al. 2013. Synthesis, Surface Modification and Characterisation of Biocompatible Magnetic Iron Oxide Nanoparticles for Biomedical Applications. *Molecules.* 18(7): 7533-7548. <https://doi.org/10.3390/molecules18077533>.
- [11] P. Biehl, M. von der Lühe, S. Dutz, and F. H. Schacher. 2018. Synthesis, Characterization, and Applications of Magnetic Nanoparticles Featuring Polyzwitterionic Coatings. *Polymers (Basel).* 10(1). <https://doi.org/10.3390/polym10010091>.
- [12] R. M. Robinson, M. Abdelmoula, M. Mallet, and R. Coustel. 2019. Starch Functionalized Magnetite Nanoparticles: New Insight into the Structural and Magnetic Properties. *J. Solid State Chem.* 277(June): 587-593. <https://doi.org/10.1016/j.jssc.2019.06.033>.
- [13] S. A. Junejo, B. M. Flanagan, B. Zhang, and S. Dhital. 2022. Starch Structure and Nutritional Functionality - Past Revelations and Future Prospects. *Carbohydr. Polym.* 277(August 2021): 118837. <https://doi.org/10.1016/j.carbpol.2021.118837>.
- [14] Y. Fan and F. Picchioni. 2020. Modification of Starch: A Review on the Application of 'Green' Solvents and Controlled Functionalization. *Carbohydr. Polym.* 241(April). <https://doi.org/10.1016/j.carbpol.2020.116350>.
- [15] X. Qiu, Y. Wang, Y. Xue, W. Li, and Y. Hu. 2020. Laccase Immobilized on Magnetic Nanoparticles Modified by Amino-functionalized Ionic Liquid via Dialdehyde Starch for Phenolic Compounds Biodegradation. *Chem. Eng. J.* 391. <https://doi.org/10.1016/j.cej.2019.123564>.
- [16] A. A. Kadam et al. 2020. Thiolation of Chitosan Loaded over Super-magnetic Halloysite Nanotubes for Enhanced Laccase Immobilization. *Nanomaterials.* 10(12): 1-20. <https://doi.org/10.1038/s41598-018-35633-8>.

- <https://doi.org/10.3390/nano10122560>.
- [17] N. A. Samak et al. 2018. CotA Laccase Immobilized on Functionalized Magnetic Graphene Oxide Nano-sheets for Efficient Biocatalysis. *Mol. Catal.* 445: 269-278. <https://doi.org/10.1016/j.mcat.2017.12.004>.
- [18] E. Steen Redeker, D. T. Ta, D. Cortens, B. Billen, W. Guedens, and P. Adriaensens. 2013. Protein Engineering for Directed Immobilization. *Bioconj. Chem.* 24(11): 1761-1777. <https://doi.org/10.1021/bc4002823>.
- [19] T. Sulistyarningsih, J. S. Santosa, D. Siswanta, and B. Rusdjarso. 2017. Synthesis and Characterization of Magnetites Obtained from Mechanically and Sonochemically Assisted Co-precipitation and Reverse Co-precipitation Methods. *Int. J. Mater. Mech. Manuf.* 5(1): 16-19. <https://doi.org/10.18178/ijmmm.2017.5.1.280>.
- [20] H. C. Roth, S. P. Schwaminger, M. Schindler, F. E. Wagner, and S. Berensmeier. 2015. Influencing Factors in the Co-precipitation Process of Superparamagnetic Iron Oxide Nano Particles: A Model-based Study. *J. Magn. Magn. Mater.* 377: 81-89. <https://doi.org/10.1016/j.jmmm.2014.10.074>.
- [21] M. Harada, M. Kuwa, R. Sato, T. Teranishi, M. Takahashi, and S. Maenosono. 2020. Cation Distribution in Monodispersed  $MFe_2O_4$  (M = Mn, Fe, Co, Ni, and Zn) Nanoparticles Investigated by X-ray Absorption Fine Structure Spectroscopy: Implications for Magnetic Data Storage Catalysts, Sensors, and Ferrofluids. *ACS Appl. Nano Mater.* 3(8): 8389-8402. <https://doi.org/10.1021/acsanm.0c01810>.
- [22] I. Sharifi, H. Shokrollahi, M. M. Doroodmand, and R. Safi. 2012. Magnetic and Structural Studies on  $CoFe_2O_4$  Nanoparticles Synthesized by Co-precipitation, Normal Micelles and Reverse Micelles Methods. *J. Magn. Magn. Mater.* 324(10): 1854-1861. <https://doi.org/10.1016/j.jmmm.2012.01.015>.
- [23] N. Mizutani, T. Iwasaki, S. Watano, T. Yanagida, H. Tanaka, and T. Kawai. 2008. Effect of Ferrous/ferric Ions Molar Ratio on Reaction Mechanism for Hydrothermal Synthesis of Magnetite Nanoparticles. *Bull. Mater. Sci.* 31(5): 713-717. <https://doi.org/10.1007/s12034-008-0112-3>.
- [24] I. K. Ghosh, Z. Iqbal, S. Bhattacharya, and A. Bordoloi. 2020. Insight of Boron Induced Single-step Synthesis of Short-chain Olefins from Bio-derived Syngas. *Fuel.* 263(November): 116663. <https://doi.org/10.1016/j.fuel.2019.116663>.
- [25] H. Jia et al. 2016. Immobilization of  $\omega$ -transaminase by Magnetic PVA- $Fe_3O_4$  Nanoparticles. *Biotechnol. Reports.* 10: 49-55. <https://doi.org/10.1016/j.btre.2016.03.004>.
- [26] S. Altun, B. Çakiroğlu, M. Özacar, and M. Özacar. 2015. A Facile and Effective Immobilization of Glucose Oxidase on Tannic Acid Modified  $CoFe_2O_4$  Magnetic Nanoparticles. *Colloids Surfaces B Biointerfaces.* 136: 963-970. <https://doi.org/10.1016/j.colsurfb.2015.10.053>.
- [27] T. Tarhan, A. Ulu, M. Sariçam, M. Çulha, and B. Ates. 2020. Maltose Functionalized Magnetic Core/shell  $Fe_3O_4@Au$  Nanoparticles for an Efficient L-asparaginase Immobilization. *Int. J. Biol. Macromol.* 142: 443-451. <https://doi.org/10.1016/j.ijbiomac.2019.09.116>.
- [28] J. Lu, Y. Li, H. Zhu, and G. Shi. 2021.  $SiO_2$ -Coated  $Fe_3O_4$  Nanoparticle/Polyacrylonitrile Beads for One-step Lipase Immobilization. *ACS Appl. Nano Mater.* 4(8): 7856-7869. <https://doi.org/10.1021/acsanm.1c01181>.
- [29] H. Peidayesh, Z. Ahmadi, H. A. Khonakdar, M. Abdous, and I. Chodák. 2020. Fabrication and Properties of Thermoplastic Starch/montmorillonite Composite using Dialdehyde Starch as a Crosslinker. *Polym. Int.* 69(3): 317-327. <https://doi.org/10.1002/pi.5955>.
- [30] J. Yu, P. R. Chang, and X. Ma. 2010. The Preparation and Properties of Dialdehyde Starch and Thermoplastic Dialdehyde Starch. *Carbohydr. Polym.* 79(2): 296-300. <https://doi.org/10.1016/j.carbpol.2009.08.005>.
- [31] M. R. Saboktakin, A. Maharramov, and M. A. Ramazanov. 2009. Synthesis and Characterization of Superparamagnetic Nanoparticles Coated with Carboxymethyl Starch (CMS) for Magnetic Resonance Imaging Technique. *Carbohydr. Polym.* 78(2): 292-295. <https://doi.org/10.1016/j.carbpol.2009.03.042>.
- [32] Y. Zuo, W. Liu, J. Xiao, X. Zhao, Y. Zhu, and Y. Wu. 2017. Preparation and Characterization of Dialdehyde Starch by One-step Acid Hydrolysis and Oxidation. *Int. J. Biol. Macromol.* 103: 1257-1264. <https://doi.org/10.1016/j.ijbiomac.2017.05.188>.
- [33] S. Das and M. K. Das. 2019. Synthesis and Characterization of Thiolated Jackfruit Seed Starch as a Colonic Drug Delivery Carrier. *Int. J. Appl. Pharm.* 11(3): 53-62. <https://doi.org/10.22159/ijap.2019v11i3.31895>.
- [34] S. Li, J. M. V. Mujiyambereb, and M. Liu. 2011. Synthesis of Carboxymethyl Starch with High Degree of Substitution by a Modified Dry Process. *Adv. Mater. Res.* 233-235(August): 306-310. <https://doi.org/10.4028/www.scientific.net/AMR.233-235.306>.
- [35] T. T. Dung, T. M. Danh, L. T. M. Hoa, D. M. Chien, and N. H. Duc. 2009. Structural and Magnetic Properties of Starch-coated Magnetite Nanoparticles. *J. Exp. Nanosci.* 4(3): 259-267. <https://doi.org/10.1080/17458080802570609>.
- [36] A. Díaz-Hernández, J. Gracida, B. E. García-Almendárez, C. Regalado, R. Núñez, and A. Amaro-Reyes. 2018. Characterization of Magnetic Nanoparticles Coated with Chitosan: A Potential Approach for Enzyme Immobilization. *J. Nanomater.* 2018. <https://doi.org/10.1155/2018/9468574>.
- [37] F. Gao and G. Ma. 2012. Effects of Microenvironment on Supported Enzymes. *Top Catal.* 55: 1114-1123. <https://doi.org/10.1007/s11244-012-9902-3>.
- [38] D.-H. Zhang, L.-X. Yuwen, and L.-J. Peng. 2013. Parameters Affecting the Performance of Immobilized Enzyme. *J. Chem.* 2013: 1-7. <https://doi.org/10.1155/2013/946248>.
- [39] C. Zhang and X. Cai. 2019. Immobilization of Horseradish Peroxidase on  $Fe_3O_4$ /nanotubes Composites for Biocatalysis-degradation of Phenol. *Compos. Interfaces.* 26(5): 379-396. <https://doi.org/10.1080/09276440.2018.1504265>.
- [40] C. Algieri, L. Donato, and L. Giorno. 2016. Tyrosinase Immobilized on a Hydrophobic Membrane. *Biotechnol. Appl. Biochem.* 1-8. <https://doi.org/10.1002/bab.1462>.
- [41] S. A. Mohamed, M. H. Al-Harbi, Y. Q. Almulaiky, I. H. Ibrahim, and R. M. El-Shishtawy. 2017. Immobilization of Horseradish Peroxidase on  $Fe_3O_4$  Magnetic Nanoparticles. *Electron. J. Biotechnol.* 27: 84-90. <https://doi.org/10.1016/j.ejbt.2017.03.010>.
- [42] N. Jailani, N. R. Jaafar, S. Suhaimi, M. M. Mackeen, F. D. A. Bakar, and R. M. Illias. 2022. Cross-linked Cyclodextrin Glucanotransferase Aggregates from *Bacillus lehensis* G1 for Cyclodextrin Production: Molecular Modeling, Developmental, Physicochemical, Kinetic and Thermodynamic Properties. *Int. J. Biol. Macromol.* 213(May): 516-533. <https://doi.org/10.1016/j.ijbiomac.2022.05.170>.
- [43] M. Bilal, M. Asgher, H. Cheng, Y. Yan, and H. M. N. Iqbal. 2019. Multi-point Enzyme Immobilization, Surface Chemistry, and Novel Platforms: A Paradigm Shift in Biocatalyst Design. *Crit. Rev. Biotechnol.* 39(2): 202-219. <https://doi.org/10.1080/07388551.2018.1531822>.
- [44] J. C. Y. Wu, C. H. Hutchings, M. J. Lindsay, C. J. Werner, and B. C. Bundy. 2015. Enhanced Enzyme Stability Through Site-Directed Covalent Immobilization. *J. Biotechnol.* 193: 83-90. <https://doi.org/10.1016/j.jbiotec.2014.10.039>.
- [45] C. C. S. Fortes, A. L. Daniel-da-Silva, A. M. R. B. Xavier, and A. P. M. Tavares. 2017. Optimization of Enzyme

- Immobilization on Functionalized Magnetic Nanoparticles for Laccase Biocatalytic Reactions. *Chem. Eng. Process. Process Intensif.* 117(August): 1-8.  
<https://doi.org/10.1016/j.cep.2017.03.009>.
- [46] X. Chen, B. He, M. Feng, D. Zhao, and J. Sun. 2020. Immobilized Laccase on Magnetic Nanoparticles for Enhanced Lignin Model Compounds Degradation. *Chinese J. Chem. Eng.* 28(8): 2152-2159.  
<https://doi.org/10.1016/j.cjche.2020.02.028>.
- [47] S. Talekar, S. Nadar, A. Joshi, and G. Joshi. 2014. Pectin Cross-linked Enzyme Aggregates (pectin-CLEAs) of Glucoamylase. *RSC Adv.* 4(103): 59444-59453.  
<https://doi.org/10.1039/C4RA09552A>.
- [48] J. O. Park, K. Y. Rhee, and S. J. Park. 2010. Silane Treatment of Fe<sub>3</sub>O<sub>4</sub> and Its Effect on the Magnetic and Wear Properties of Fe<sub>3</sub>O<sub>4</sub> /epoxy Nanocomposites. *Appl. Surf. Sci.* 256(23): 6945-6950.  
<https://doi.org/10.1016/j.apsusc.2010.04.110>.
- [49] S. Anjum, T. Zeeshan, S. Waseem, I. Waseem, and Z. Mustafaz. 2022. Investigation of Cationic Distribution, Y-K Angles, and Optical and Dielectric Properties of as-synthesized Cerium-doped Cobalt nano-ferrites Prepared by Co-precipitation Method. *Appl. Phys. A Mater. Sci. Process.* 128(5): 1-13.  
<https://doi.org/10.1007/s00339-022-05470-8>.
- [50] S. Asmat, Q. Husain, and M. S. Khan. 2018. A Polypyrrole-methyl Anthranilate Functionalized Worm-like Titanium Dioxide Nanocomposite as an Innovative Tool for Immobilization of Lipase: Preparation, Activity, Stability and Molecular Docking Investigations. *New J. Chem.* 42(1): 91-102.  
<https://doi.org/10.1039/C7NJ02951A>.
- [51] A. Rajan, J. D. Sudha, and T. E. Abraham. 2008. Enzymatic Modification of Cassava Starch by Fungal Lipase. *Ind. Crops Prod.* 27(1): 50-59.  
<https://doi.org/10.1016/j.indcrop.2007.07.003>.
- [52] Z. Wang et al. 2021. The Study of Laccase Immobilization Optimization and Stability Improvement on CTAB-KOH Modified Biochar. *BMC Biotechnol.* 21(1): 1-14.  
<https://doi.org/10.1186/s12896-021-00709-3>.
- [53] J. Xu et al. 2013. Synthesis and Characterization of Magnetic Nanoparticles and Its Application in Lipase Immobilization. *Bull. Korean Chem. Soc.* 34(8): 2408-2412.  
<https://doi.org/10.5012/bkcs.2013.34.8.2408>.
- [54] A. Ali et al. 2021. Review on Recent Progress in Magnetic Nanoparticles: Synthesis, Characterization, and Diverse Applications. *Front. Chem.* 9(July): 1-25.  
<https://doi.org/10.3389/fchem.2021.629054>.